

Biomimetic Model of Coenzyme B₁₂: Aquabis(ethane-1,2-diamine- $\kappa N, \kappa N'$)ethylcobalt(III) – Its Kinetic and Binding Studies with Imidazoles and Amino Acids and Interactions with CT DNA

by **Ponuganti Pallavi, Penumaka Nagababu, and Sirasani Satyanarayana***

Department of Chemistry, Osmania University, Hyderabad, 500007, India
(phone: +91-40-27682337; e-mail: ssnirasani@yahoo.com)

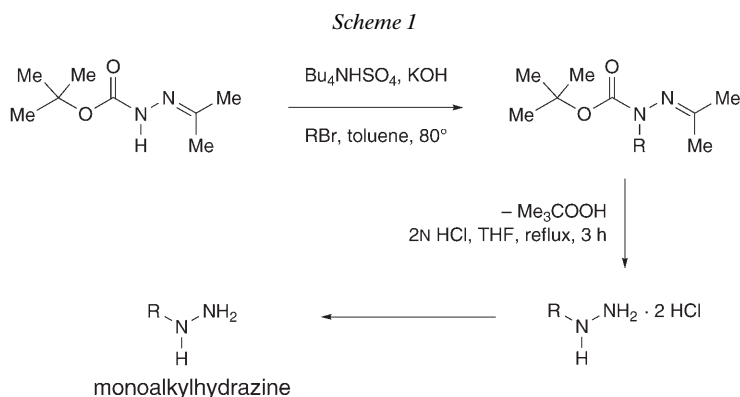
Pseudo-first-order reaction kinetics and binding studies of *trans*-[Co(en)₂(Et)H₂O] complex with 1*H*-imidazole, substituted 1*H*-imidazoles, histidine, histamine, glycine and glycine ethyl ester were investigated by means of spectrophotometric techniques. Equilibrium constants were determined as a function of pH at 25°. Binding and kinetic studies were correlated to basicity and steric hindrance. From the equilibrium data, it was found that the entering nucleophile is participating in the transition state, an I_a mechanism is proposed. The effect of the incoming ligands on the complex was studied by molecular mechanics. The interaction of *trans*-[Co(en)₂(Et)H₂O] with CT DNA was studied spectrophotometrically.

Introduction. – To understand the mechanistic aspect of coenzyme B₁₂, which actively carries many enzymatic reactions, model complexes of the coenzyme are widely studied. Much of the study with model complexes reveals that the active part of the coenzyme is the Co–C bond cleavage, which initiates the enzymatic reaction. The pentammine(methyl)cobalt(III) complex is the simplest model for coenzyme B₁₂ [1], where four ammine ligands are bound to the Co-center in equatorial positions and one ammine and the methyl ligand are in axial positions *trans* to each other. Later, cobalamins and cobaloximes were extensively studied.

The carbanion ligand coordinated to the Co^{III} center is influenced by the presence of other ligands in *cis* or *trans* position with respect to the carbanion ligand. A *cis* and *trans* effect on the Co–C bond was reported for naturally occurring methylcobalamin [2] and various synthetic complexes such as those with tetrapyrrole, imine, oxime, mixed imine-oxime or ammine ligands [3–7]. The data for the *trans*-[Co(DH)₂(Me)L] (DH = dmg = dimethylglyoximate) revealed that the ¹³C-NMR chemical shift, the ⁵⁹Co¹³C coupling constant [8], and the bond distance are influenced by the *trans* ligand [9]. We have previously studied the *trans* influence in cobaloxime (= bis{[butane-2,3-dione di(oximate- κN)](1–)}cobalt(III)) with varying ligands using spectrophotometric methods and molecular mechanics [10]. Now, we report the *trans* and *cis* influence of ligands on *trans*-[Co(en)₂(Et)OH₂] (en = ethane-1,2-diamine) based on the kinetic and binding studies.

Experimental. – *General.* *tert*-Butyl carbazate (= *tert*-butyl hydrazinecarboxylate), acetone, bromoethane, histidine, histamine, 1*H*-imidazole, 1-methyl-1*H*-imidazole, 2-methyl-1*H*-imidazole, 1,2-dimethyl-1*H*-imidazole, glycine, and glycine ethyl ester were purchased from *Sigma-Aldrich Chemicals*.

Tetrabutylammonium hydrogen sulfate ($\text{Bu}_4\text{N}(\text{HSO}_4)$), KOH, MgSO_4 , conc. HCl soln., $\text{Co}(\text{NO}_3)_3$, ammonia soln., and MeOH were obtained from *Merck*. Ethylhydrazine was prepared according to [11] and *Scheme 1* as it is used as alkylating agent. pH Measurements: *Digisun DI-707* pH meter calibrated with standard buffers of pH 4.0, 7.0, and 9.2. UV/VIS Spectra: *Elico BL-198* spectrophotometer with temp. control; kinetics and binding studies with an *Elico SL-171* single-beam spectrophotometer. IR Spectra: *Perkin-Elmer 1600* FT-IR spectrophotometer.



(OC-6-32)-*Aquabis(ethane-1,2-diamine-κN,κN')ethyl cobalt(III)* (*trans*- $[\text{Co}(\text{en})_2(\text{Et})\text{OH}_2]$) was prepared according to [1][7b] with ethylhydrazine (R = Et in *Scheme 1*). ^1H - and ^{13}C -NMR: *Fig. 1*.

Binding and Kinetic Studies. The binding and kinetic studies were carried out by the *Elico SL-171* single-beam spectrophotometer. Spectra were recorded with a *Hitachi U-3410*. The concentrations were fixed at 456 nm. The sample-compartment temp. was maintained at $25^\circ \pm 1^\circ$.

Determination of Equilibrium Constants. The apparent binding constants (K_{app}) were determined for the axial ligation of the *trans*- $[\text{Co}(\text{en})_2(\text{Et})\text{OH}_2]$ complex with different ligands. By taking a fixed concentration of complex and varying the ligand concentration, the absorbance was recorded. For this, solns. containing an appropriate buffer (0.2M) to maintain pH, KCl to maintain ionic strength (1.0M), and varying concentrations of ligand in a 3-ml cuvette were allowed to equilibrate in a thermostat cell holder at $25 \pm 0.1^\circ$ for 15 min prior to addition of *trans*- $[\text{Co}(\text{en})_2(\text{Et})\text{OH}_2]$.

The apparent equilibrium constants were calculated from the plot of $\Delta A/[L]_f$ vs. ΔA . Thus, for each ligand, K_{app} was calculated by *Eqn. 1*. The least square fit for *Eqn. 1*, after rearrangement, is given by *Eqn. 2*, where ΔA is the difference in absorbance between solns. containing only complex with and without ligand, ΔA_{max} is the maximum difference in absorbance recorded at high ligand concentration and $[L]_f$ is the unbound ligand concentration which is calculated from *Eqn. 3*. In *Eqn. 3*, $[L]_T$ is the total volume of ligand added, and C_T is the total concentration of *trans*- $[\text{Co}(\text{en})_2(\text{Et})\text{OH}_2]$.

$$\Delta A = \Delta A_{\text{max}} [L]_f / (1/K_{\text{app}} + [L]_f) \quad (1)$$

$$\Delta A = \Delta A_{\text{max}} - \{1/K_{\text{app}} (\Delta A/[L]_f)\} \quad (2)$$

$$[L]_f = [L]_T - (C_T \Delta A / \Delta A_{\text{max}}) \quad (3)$$

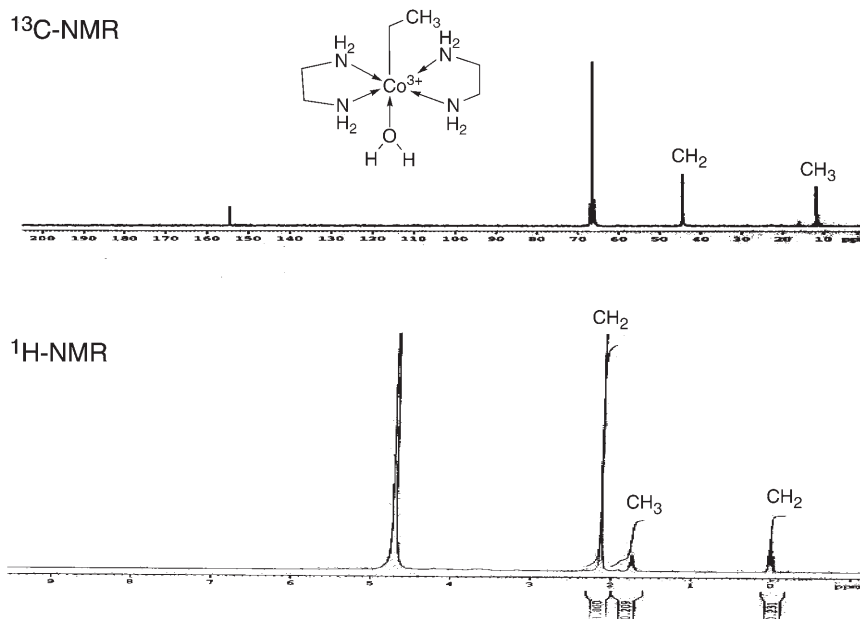


Fig. 1. ^1H - and ^{13}C -NMR Spectra of the aquabis(ethane-1,2-diamine)ethylcobalt(III) complex

The pH-independent equilibrium constants are then calculated from Eqn. 4, where α_L (fraction of ligand as free base) is determined from Eqn. 5:

$$K_{\text{eq}} = K_{\text{app}}/\alpha_L \quad (4)$$

$$\alpha_L = K_a/(K_a + [\text{H}^+]) \quad (5)$$

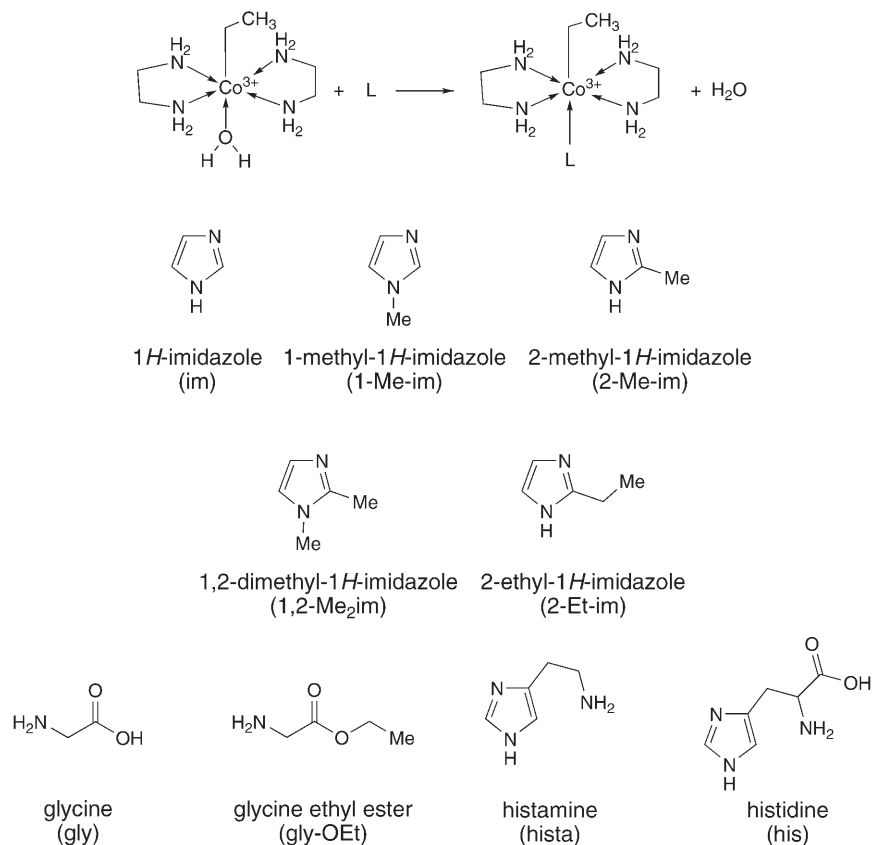
Kinetic Studies. We investigated the ligand-substitution reactions of *trans*-[Co(en)₂(Et)OH₂] with 1*H*-imidazole and substituted 1*H*-imidazoles at 25°. The reaction rates were determined by maintaining pseudo-first-order conditions by taking a 10-fold excess of ligand concentration with respect to the complex concentration. The kinetics was studied by varying the concentration of the ligand at 456 nm and by using an appropriate buffer at a pH below the p*K*_a of the ligand. The absorbance was monitored at λ_{max} 456 nm. The first-order rate constants (*k*_{obs}) were obtained by least-square fits of the data to Eqn. 6, where *A*_{*t*} is the absorbance at time '*t*', and *A*_∞ is the final absorbance.

$$\ln A_t - \ln A_\infty = k_{\text{obs}}t \quad (6)$$

Results and Discussion. – The ligand-substitution reaction of *trans*-[Co(en)₂(Et)OH₂] with 1*H*-imidazole (im), substituted 1*H*-imidazoles, histidine (his), histamine (hista), glycine (gly) and glycine ethyl ester (gly-OEt) is shown in Scheme 2.

The UV/VIS scan of *trans*-[Co(en)₂(Et)OH₂] is given in Fig. 2. Fig. 3 shows the variation of the absorption spectrum of the complex in the presence of different concentrations of the ligand 1-methyl-1*H*-imidazole (1-Me-im). Depending on the p*K*_a

Scheme 2



values of the ligands, the binding studies were performed in the pH range above and below the $\text{p}K_{\text{a}}$ values. The K_{app} values for ligation of *trans*-[Co(en)₂(Et)OH₂]³⁺ with 1*H*-imidazoles were determined as a function of pH by spectrophotometry (see Fig. 4 and Table I). Up to the $\text{p}K_{\text{a}}$ of the ligand, $\log K_{\text{app}}$ increases with pH, but above $\text{p}K_{\text{a}}$, $\log K_{\text{app}}$ is independent of pH. The K_{app} value below the $\text{p}K_{\text{a}}$ value is very low due to the protonation of the ligand, but as the pH increases, the ligand is deprotonated and binds strongly to Co^{III}, thus K_{app} increases. The affinities of the ligands follow the order: 1-Me-im > im > 2-Me-im > 1,2-Me₂im > 2-Et-im. Among the amino acids, the order is: histidine > histamine > glycine > glycine ethyl ester.

The stability order can be explained by considering the HSAB principle, basicity of the ligands, and their ability of π -bonding and σ -donation. In the 1*H*-imidazole series, the formation constants for 1-Me-im and im are high, and they follow the basicity order. From 2-Me-im to 2-Et-im, steric hindrance at C(2) of the 1*H*-imidazole plays a role, thus these ligands do not follow the basicity order. In the amino acid series, there is no increase in K_{app} at pH above the $\text{p}K_{\text{a}}$ of the ligands histamine and histidine indicating

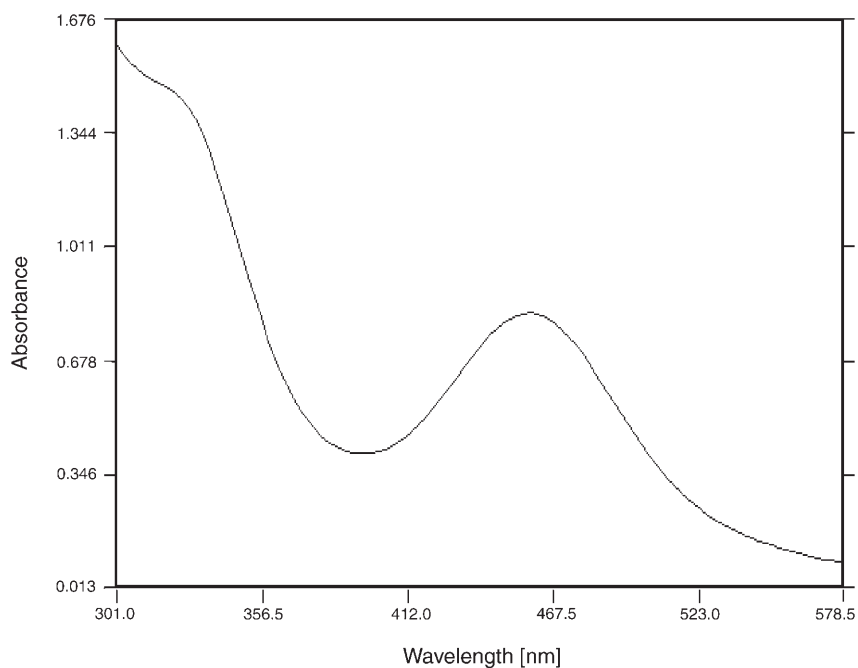


Fig. 2. UV/VIS Absorption spectra of the aquabis(ethane-1,2-diamine)ethylcobalt(III) complex showing λ_{\max} at 456 nm

that binding is through the endocyclic N-atom. Though histamine is slightly more basic than histidine, histidine forms a more stable complex as it is a better π -acceptor than histamine. Glycine and glycine ethyl ester, are both σ -donors, but glycine has a higher binding constant as it is more basic than glycine ethyl ester. The stability order of the complexes is attributed to the ability of the 1*H*-imidazoles, histidine, or histamine to accept electrons into higher-energy unfilled π^* anti-bonding orbitals through $d\pi - p\pi$ back bonding. Glycine and glycine ethyl ester cannot accept electrons in a similar way.

The rate of ligand substitution is pH-dependent, which is shown in Fig. 5. The rate of the reaction increases drastically near the pK_a of the ligand. The slope of the plot of k_{obs} vs. concentration of the ligand given in Fig. 6 gives the second order rate constant k'_{on} at a given pH. The data for the plot is given in Table 2. The slopes of the least-square fit of Eqn. 7 gives the second-order rate constant, where $[L]_{\text{T}}$ is the total ligand concentration. The pH independent second-order rate constants k_{on} are obtained by using Eqn. 8. The plot of k_{obs} vs. pH given in Fig. 5 clearly indicates that as the pH increases, k_{obs} increases as the deprotonated form of the ligand is readily available at higher pH.

$$k_{\text{obs}} = k'_{\text{on}} [L]_{\text{T}} + k_{\text{off}} \quad (7)$$

$$k_{\text{on}} = k'_{\text{on}} / \alpha_{\text{L}} \quad (8)$$

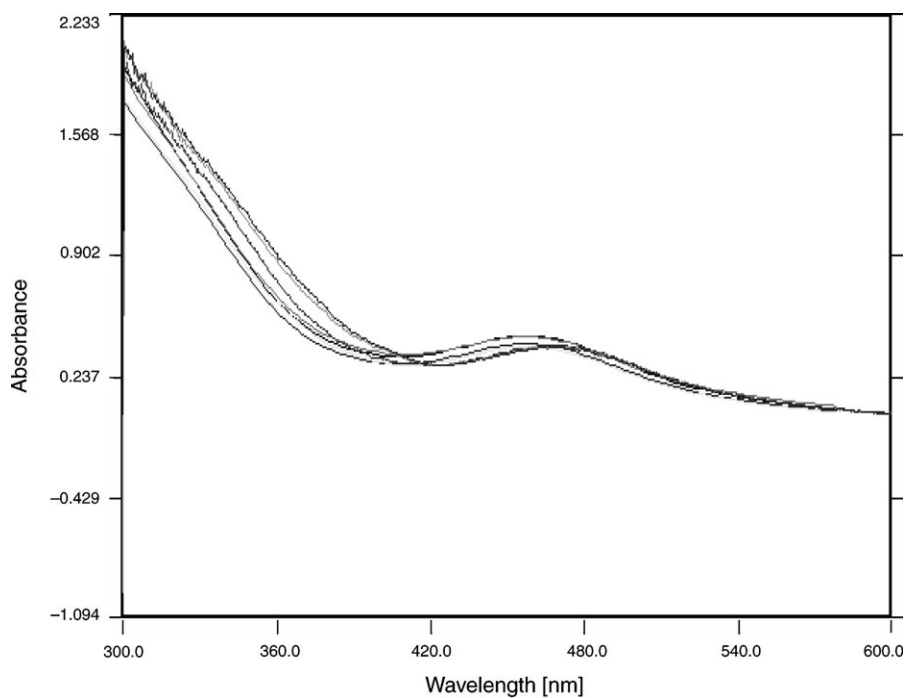


Fig. 3. UV/VIS Scan: Binding of the aquabis(ethane-1,2-diamine)ethylcobalt(III) complex with varying concentrations of 1-methyl-1H-imidazole at pH 6 and 25°. Isosbestic point at 470 and 400 nm.

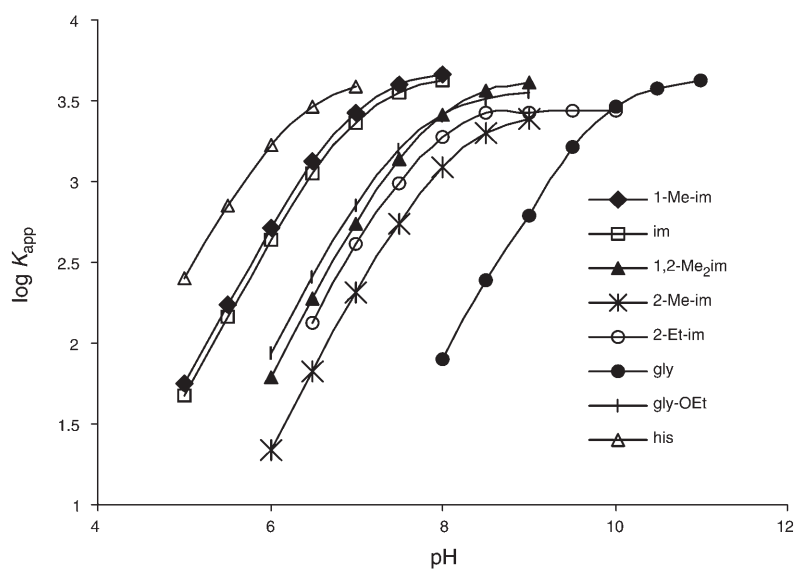
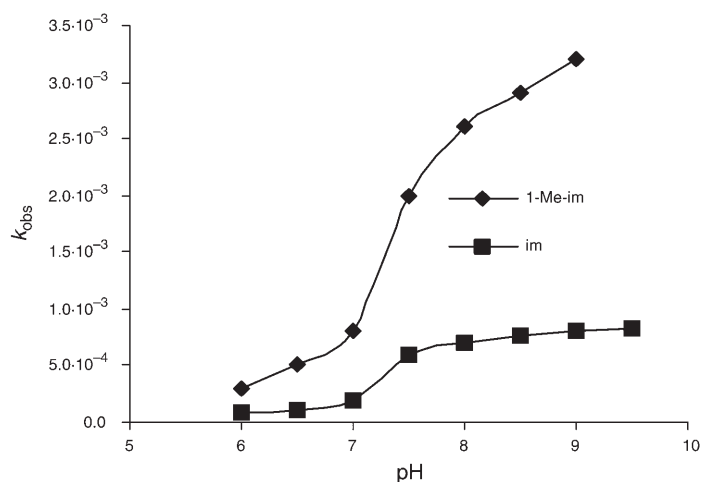


Fig. 4. Dependence of the formation constants, $\log K_{app}$ on the pH for the axial ligation of the aquabis(ethane-1,2-diamine)ethylcobalt(III) complex by different ligands at 25°

Table 1. Formation Constants ($\log K_{\text{app}}$) for the Axial Ligation of the Aquabis(ethane-1,2-diamine)ethylcobalt(III) Complex by Different Ligands at 25° for Different pH Values

pH	1-Me-im	im	1,2-Me ₂ im	2-Me-im	2-Et-im	gly	gly-OEt	his	hista
5.0	1.749	1.670	–	–	–	–	–	2.406	2.398
5.5	2.238	2.160	–	–	–	–	–	2.856	2.849
6.0	2.707	2.632	1.789	1.337	–	–	1.937	3.406	3.222
6.5	3.122	3.052	2.278	1.830	2.125	–	2.415	3.473	3.466
7.0	3.427	3.368	2.739	2.308	2.615	–	2.854	3.593	3.585
7.5	3.596	3.547	3.136	2.743	2.989	–	3.202	–	–
8.0	3.667	3.624	3.414	3.087	3.273	1.901	3.416	–	–
8.5	–	–	3.559	3.295	3.422	2.384	3.513	–	–
9.0	–	–	3.617	3.389	3.483	2.793	3.549	–	–
9.5	–	–	–	–	3.426	3.211	–	–	–
10.0	–	–	–	–	3.435	3.458	–	–	–
10.5	–	–	–	–	–	3.578	–	–	–
11.0	–	–	–	–	–	3.625	–	–	–
K_{eq}	5050.838	4618.62	4428.07	3652.82	2762.01	4446.92	3688.95	4578.12	4497.069

Fig. 5. Dependence of the rate constants k_{obs} on the pH for the axial ligation of aquabis(ethane-1,2-diamine)ethylcobalt(III) complex by 1H-imidazoles at 25°

The second-order rate constants increase as the nucleophilicity of the ligand increases. This is in accordance with the order of the K_{eq} values. The kinetics of substitution of axial base in alkylcobaloximes (= alkylbis[[butane-2,3-dione di(oximato- κN)](1-)]cobalt(III)) and related cobalt complexes has been studied under a variety of conditions [12][13]. The studies on cobalt complexes and adenosylcobaloxime provide evidences for the mechanism of substitution to be dissociative [13][14] (I_{d}). In view of the evidence presented above, for the existence of pentacoordinate alkylcobaloximes and the ligation kinetic studies of others, both on alkylcobalt

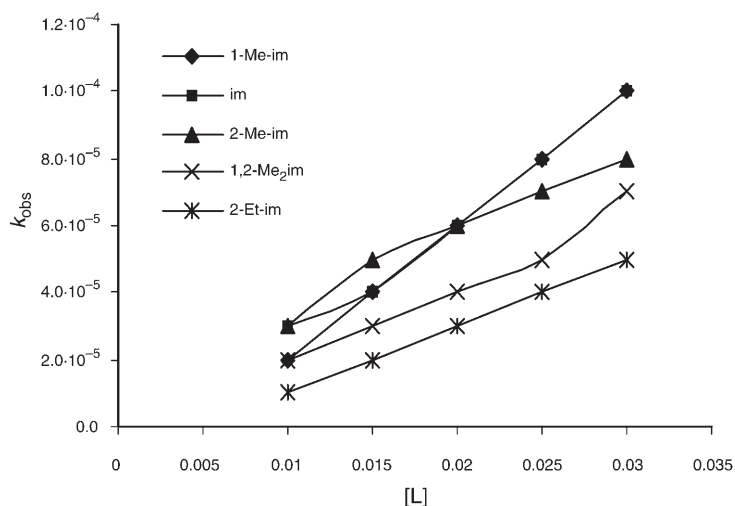


Fig. 6. Dependence of the rate constant k_{obs} on the concentration of the ligand L for the axial ligation of aquabis(ethylenediamine)ethylcobalt(III) complex by different ligands, at 25°

Table 2. Dependence of the Rate Constants, k_{obs} for the Axial Ligation of Aqua(ethane-1,2-diamine)-ethylcobalt(III) on the Concentration of the Ligand $[L]$ at 25°

	M/L	1-Me-im	im	2-Me-im	1,2-Me ₂ im	2-Et-im
k_{obs} [s ⁻¹]	1:10	$2 \cdot 10^{-5}$	$3 \cdot 10^{-5}$	$3 \cdot 10^{-5}$	$2 \cdot 10^{-5}$	$1 \cdot 10^{-5}$
	1:15	$4 \cdot 10^{-5}$	$4 \cdot 10^{-5}$	$5 \cdot 10^{-5}$	$3 \cdot 10^{-5}$	$2 \cdot 10^{-5}$
	1:20	$6 \cdot 10^{-5}$	$6 \cdot 10^{-5}$	$6 \cdot 10^{-5}$	$4 \cdot 10^{-5}$	$3 \cdot 10^{-5}$
	1:25	$8 \cdot 10^{-5}$	$8 \cdot 10^{-5}$	$7 \cdot 10^{-5}$	$5 \cdot 10^{-5}$	$4 \cdot 10^{-5}$
	1:30	$1 \cdot 10^{-4}$	$1 \cdot 10^{-4}$	$8 \cdot 10^{-5}$	$7 \cdot 10^{-5}$	$5 \cdot 10^{-5}$
k'_{on}		0.0040	0.0036	0.0026	0.0024	0.0020
pH		6.0	6.0	7.0	7.0	7.0
α		0.1013	0.11096	0.1747	0.1238	0.0736
k_{on}		0.0395	0.0324	0.0149	0.0194	0.0272

complexes and on cobaloxime complexes [15][16] with other equatorial ligand system [17], an I_d mechanism may be suggested.

Molecular-Mechanistic Studies. The structural investigation of coordination and organometallic chemistry has been boosted by using molecular mechanics [18–21]. By means of MM2 parameterization, the optimized structures resulting from axial ligation of $[\text{Co}(\text{en})_2(\text{Et})\text{OH}_2]$ by different ligands were calculated with Bio Med CA Cache 5.02 software. Fig. 7 shows a ball-and-stick representation of the complex with ethyl-1*H*-imidazole. The calculated bond lengths and bond strains are given in Table 3.

DNA Binding. Absorption Spectral Studies. The application of electronic absorption spectroscopy in DNA-binding studies is one of the most useful techniques [22–23]. Complex binding with DNA in the groove mode usually results in hypochromism and bathochromism, due to the groove mode involving a strong stacking interaction

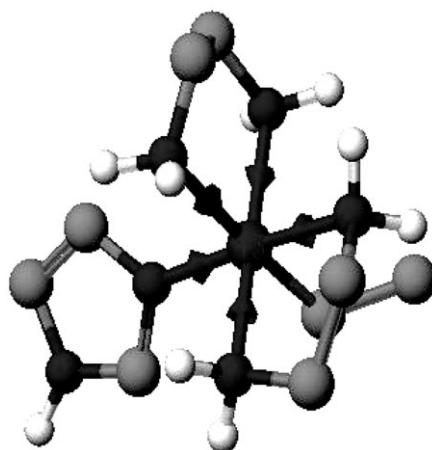


Fig. 7. Ball-and-stick representation of the minimum-energy structure of $[Co(en)_2(Et)OH_2]$. Center dark grey, Co-center; light grey, C-atoms; dark grey, N-atoms; white, H-atoms.

Table 3. Bond Lengths [\AA] and Bond-Strain Values (parentheses [\AA]) Obtained from Molecular-Mechanics Studies with *trans*-Aquabis(ethane-1,2-diamine)ethylcobalt(III) Complex and Different Ligands

Ligand	Co–N(1)	Co–N(1)	Co–N(1)	Co–N(1)	Co–C	Co–N	Co–O
H ₂ O	2.162 (0.033)	2.162 (0.069)	2.162 (0.039)	2.161 (0.050)	1.930 (0.116)	–	1.890 (0.191)
hist	2.170 (0.018)	2.174 (0.004)	2.167 (0.037)	2.172 (0.011)	1.954 (0.182)	1.933 (0.092)	–
hista	2.170 (0.018)	2.174 (0.003)	2.167 (0.038)	2.171 (0.011)	1.954 (0.191)	1.933 (0.096)	–
gly	2.171 (0.016)	2.174 (0.004)	2.174 (0.006)	2.169 (0.022)	1.954 (0.183)	1.934 (0.103)	–
gly-OEt	2.170 (0.019)	2.174 (0.005)	2.173 (0.007)	2.169 (0.023)	1.954 (0.177)	1.933 (0.085)	–
im	2.169 (0.022)	2.174 (0.004)	2.167 (0.035)	2.171 (0.012)	1.955 (0.196)	1.935 (0.108)	–
1-Me-im	2.169 (0.021)	2.173 (0.004)	2.167 (0.034)	2.171 (0.013)	1.955 (0.197)	1.934 (0.110)	–
2-Me-im	2.172 (0.008)	2.176 (0.001)	2.168 (0.026)	2.172 (0.009)	1.954 (0.179)	1.950 (0.352)	–
1,2-Me ₂ im	2.173 (0.007)	2.175 (0.002)	2.168 (0.026)	2.172 (0.008)	1.954 (0.195)	1.950 (0.360)	–
2-Et-im	2.168 (0.025)	2.177 (0.000)	2.170 (0.017)	2.170 (0.016)	1.949 (0.113)	1.959 (0.593)	–

between an aromatic chromophore and the base pairs of DNA. The extent of the hypochromism commonly parallels the groove binding strength. The absorption spectra of the complex $[Co(en)_2(Et)OH_2]$ in the absence and presence of calf thymus DNA in

Tris buffer are illustrated in Fig. 8. In the UV region, the intense absorption bands observed for Co^{III} complexes are attributed to intraligand $\pi-\pi^*$ transition of the coordinated groups. Addition of increasing amounts of CT DNA results in hypochromism and a moderate bathochromic shift of the UV spectrum of the complex $[\text{Co}(\text{en})_2(\text{Et})\text{OH}_2]$. These spectral data may suggest a mode of binding that involves a stacking interaction between the complex and the base pairs of DNA. To quantitatively determine binding strength of the Co^{III} complex, the intrinsic binding constants K of the complex with CT DNA were determined according to Eqn. 9 [24] through a plot of $[\text{DNA}]/(\Sigma_b - \Sigma_f)$ vs. $[\text{DNA}]$, where $[\text{DNA}]$ is the concentration of DNA in base pairs. The apparent absorption coefficients Σ_a , Σ_f and Σ_b correspond to $A_{\text{obs}}/[\text{Co}]$, and to the extinction coefficient for the Co^{III} complex in the free and fully bound form, respectively. In the plots $[\text{DNA}]/(\Sigma_b - \Sigma_f)$ vs. $[\text{DNA}]$, K is given by the ratio of slope to intercept. Intrinsic binding constants K of ca. $3.3 \pm 0.2 \cdot 10^3 \text{ M}^{-1}$ were obtained from the decay of the absorbance. The binding constants indicate that the complex binds strongly to the DNA.

$$[\text{DNA}]/(\Sigma_a - \Sigma_f) = [\text{DNA}]/(\Sigma_b - \Sigma_f) + 1/(K (\Sigma_b - \Sigma_f)) \quad (9)$$

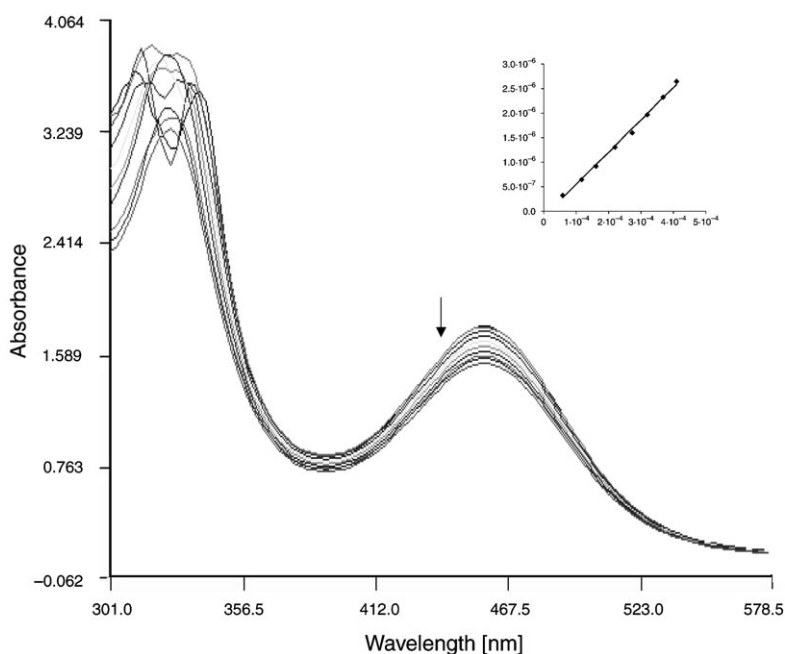


Fig. 8. Absorption spectra of $[\text{Co}(\text{en})_2(\text{Et})\text{OH}_2]$ (top) in the absence of CT DNA, the absorbance changing upon increasing CT DNA concentrations. The arrow shows the intensity change upon increasing DNA concentration. The complex exhibits hypochromicity during the absorption titration experiment with CT DNA. Inset: experimental data points (\blacklozenge) of $[\text{DNA}]/(\Sigma_a - \Sigma_f)$ vs. $[\text{DNA}]$ for the titration of complex with DNA (Eqn. 9); solid line, linear fitting of the data.

Fluorescence Spectroscopic Studies. The complex $[\text{Co}(\text{en})_2(\text{Et})\text{OH}_2]$, exhibits luminescence in *Tris* buffer (pH 7.0) at room temperature with a maximum at 555 nm. Binding of the complex to DNA was found to increase the fluorescence intensity. The emission spectra of the complex in the absence and presence of CT DNA are shown in Fig. 9, besides the plot of the relative intensity vs. the ratio of $[\text{DNA}]/[\text{Co}]$ in the inset. Upon addition of CT DNA, the emission intensity increases steadily.

This observation is further supported by the emission quenching experiments with $[\text{Fe}(\text{CN})_6]^{4-}$ as quencher. The ion $[\text{Fe}(\text{CN})_6]^{4-}$ has been shown to be able to distinguish differently bound Co^{III} species, and positively charged free complex ions should be readily quenched by $[\text{Fe}(\text{CN})_6]^{4-}$. The complex bound to DNA can be protected from the quencher, because the highly negatively charged $[\text{Fe}(\text{CN})_6]^{4-}$ ions would be repelled by the negatively charged DNA phosphate backbone, thus hindering the quenching of the emission of the bound complex. The method essentially consists of titrating a given amount of DNA – metal complex by increasing the concentration of $[\text{Fe}(\text{CN})_6]^{4-}$ and measuring the change in fluorescence intensity (Fig. 9). The ferrocyanide quenching curves for this complex in the presence and absence of CT DNA are shown in (Fig. 10). Obviously, the complex inserts into DNA much deeper. The absorption and fluorescence spectroscopy studies determine the binding of the complex with DNA.

Conclusions. – The ligand-substitution reactions were studied with different ligands and *trans*-aquabis(ethane-1,2-diamine)ethyl cobalt(III). The affinities of the ligands follow the orders 1-Me-im > im > 2-Me-im > 1,2-Me₂im > 2-Et-im and histidine > histamine > glycine > glycine ethyl ester. The binding and kinetic constants varied

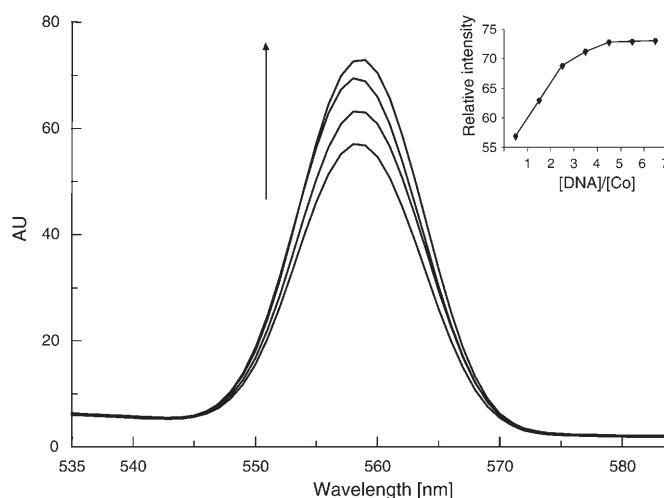


Fig. 9. Emission spectra of complex of $[\text{Co}(\text{en})_2(\text{Et})\text{OH}_2]$ in BPE buffer (pH 7.0) in the absence and presence of CT DNA. The arrow shows the intensity change upon increasing DNA concentrations. Inset: plot of the relative integrated emission intensity vs. $[\text{DNA}]/[\text{Co}]$.

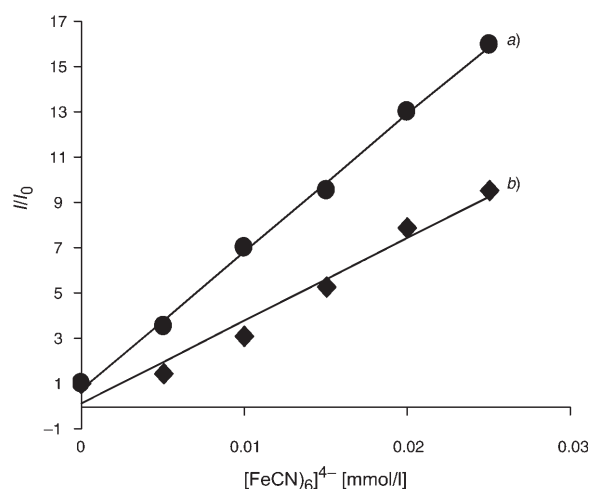


Fig. 10. Emission quenching with Co(III) complex a) without and b) with DNA. Conditions: [Co] = 2 $\mu\text{mol}/\text{cm}^{-3}$, [DNA]/[Co] = 40.

with the incoming nucleophile suggesting that the nucleophile is taking part in the transition state. Thus, an I_d mechanism is proposed. The binding studies suggest that the complex $[\text{Co}(\text{en})_2(\text{Et})\text{OH}_2]$ binds with DNA.

We gratefully acknowledge the UGC, New Delhi, for financial support in the form of major research project.

REFERENCES

- [1] P. Kofod, *Inorg. Chem.* **1995**, *34*, 2768.
- [2] 'Vitamin B₁₂ and B₁₂-Proteins', Eds. B. Kräutler, D. Arigoni, and B. T. Golding, Wiley-VCH, Weinheim, Germany, 1998.
- [3] D. Dolphin, A. W. Johnson, *J. Chem. Soc., Chem. Commun.* **1965**, 494.
- [4] K. Farmery, D. H. Busch, *Inorg. Chem.* **1972**, *11*, 2901.
- [5] G. N. Schrauzer, *Angew. Chem., Int. Ed.* **1976**, *15*, 417; B. D. Gupta, V. Vijaikanth, V. Singh, *Organometallics* **2004**, *23*, 2069; V. Vijaikanth, B. D. Gupta, D. Mandal, S. Shekhar, *Organometallics* **2005**, *24*, 4454.
- [6] G. Costa, G. Mestroni, E. de Savorgnami, *Inorg. Chim. Acta* **1969**, *3*, 323.
- [7] a) T. S. Roche, J. F. Endicott, *J. Am. Chem. Soc.* **1972**, *94*, 8622; b) P. Kofod, P. Harris, S. Larsen, *Inorg. Chem.* **1997**, *36*, 2258.
- [8] F. Asaro, L. Liguori, G. Pellizer, *Phys. Chem. Chem. Phys.* **1999**, *1*, 4981.
- [9] L. Randaccio, N. Bresciani-Pahor, E. Zangrando, L. G. Marzilli, *Chem. Soc. Rev.* **1989**, *18*, 225.
- [10] D. R. Sudharshan, B. R. Krishna, P. Pallavi, N. Navaneetha, S. Satyanarayana, *Indian J. Chem., Sect. A.* **2005**, *44*, 678; N. Navaneetha, S. Satyanarayana, *Indian J. of Chem., Sect. A.* **2005**, *44*, 1191; J. V. Madhuri, V. Malathi, S. Satyanarayana, *J. Chem. Sci.* **2004**, *116*, 143; J. V. Madhuri, V. Malathi, S. Satyanarayana, *J. Chem. Sci.* **2005**, *117*, 305.
- [11] K. G. Meyer, *Synlett* **2004**, 2355.
- [12] C. K. Poon, *Coord. Chem. Rev.* **1973**, *10*, 1.
- [13] A. W. Herlinger, T. L. Brown, *J. Am. Chem. Soc.* **1972**, *94*, 388.
- [14] P. Daublain, J. H. Horner, A. Kuznetsov, M. Newcomb, *J. Am. Chem. Soc.* **2004**, *126*, 5368.

- [15] G. Costa, G. Mestroni, G. Tauzher, D. M. Goodall, H. A. O. Hill, *J. Chem. Soc. D* **1970**, 34.
- [16] J. E. Earley, J. G. Zimmerman, *Inorg. Nucl. Chem. Lett.* **1972**, 8, 687.
- [17] J. Zsako, Z. Finta, C. S. Varhelyi, *J. Inorg. Nucl. Chem.* **1972**, 34, 2887.
- [18] N. Fey, *J. Chem. Technol. Biotechnol.* **1999**, 74, 852.
- [19] I. B. Bersukker, M. K. Leong, J. E. Boggs, R. S. Pearl Man, *Bol. Soc. Chil. Quim.* **1997**, 42, 405.
- [20] R. Cini, G. Giorgi, F. Laschi, C. Rossi, L. G. Marzilli, *J. Biomol. Struct. Dyn.* **1990**, 7, 859.
- [21] N. L. Allinger, *J. Am. Chem. Soc.* **1977**, 99, 8127.
- [22] J. M. Kelly, A. B. Tossi, D. J. McConnell, C. OhUigin, *Nucleic Acids Res.* **1985**, 13, 6017.
- [23] S. A. Tysoe, R. J. Morgan, A. D. Baker, T. C. Streckas, *J. Phys. Chem.* **1993**, 97, 1707.
- [24] A. Wolfe, G. H. Shimer, T. Meehan, *Biochemistry*, **1987**, 26, 6392.

Received July 4, 2006